Bioresource Technology 300 (2020) 122705

Contents lists available at ScienceDirect

Bioresource Technology

journal homepage: www.elsevier.com/locate/biortech

Novel biosorbents synthesized from fungal and bacterial biomass and their applications in the adsorption of volatile organic compounds

Zhuowei Cheng[a], Ke Feng[a], Yousheng Su[a], Jiexu Ye[a], Dongzhi Chen[a,*], Shihan Zhang[a], Xiaomin Zhang[a], Dionysios D. Dionysiou[b]

[a] College of Environment, Zhejiang University of Technology, Hangzhou 310009, China
[b] Environmental Engineering and Science Program, Department of Chemical and Environmental Engineering (ChEE), University of Cincinnati, Cincinnati, OH 45221-0012, USA

GRAPHICAL ABSTRACT

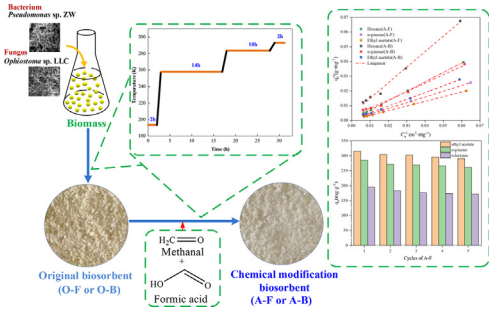

ARTICLE INFO

Keywords:
Microbial biosorbents
Fungal
VOC adsorption
Aminomethylation modification
Adsorption kinetics

ABSTRACT

Adsorption is an efficient and low-cost technology used to purify volatile organic compounds (VOCs). In the current study, novel microbial adsorbents were synthesized using cells of lyophilized fungi (*Ophiostoma stenoceras* LLC) or bacteria (*Pseudomonas veronii* ZW) that were modified by aminomethylation. Based on the adsorption performance and structural characterization results, the modified fungal biosorbent was the best. Its maximum adsorption capacities for ethyl acetate, α-pinene, and n-hexane were 620, 454, and 374 $mg \cdot g^{-1}$, respectively, which were much higher than those of other synthesized biosorbents. The specific surface area of the fungal biosorbent was 20 $m^2 \cdot g^{-1}$, and most of the components were hydrocarbon compounds and polysaccharides. The VOC adsorption process on these synthesized biosorbents was in accordance with the Langmuir isothermal model and the pseudo-first-order kinetic model, thereby suggesting that physical adsorption was the dominant mechanism. The fungal biosorbent could be used for five consecutive VOC sorption-desorption cycles without any obvious decrease in adsorption capacity.

1. Introduction

Most volatile organic compounds (VOCs) are major air pollutants emitted during industrial production and are also caused by human activities (Shen and Zhang, 2019). Some VOCs severely threaten human living conditions and health because of their toxic, mutagenic, and carcinogenic characteristics, which can cause nausea, headache, pharyngitis, and even death (Dai et al., 2017). VOCs can also react with NO_x

* Corresponding author.
E-mail address: cdz@zjut.edu.cn (D. Chen).

https://doi.org/10.1016/j.biortech.2019.122705
Received 9 November 2019; Received in revised form 25 December 2019; Accepted 26 December 2019
Available online 28 December 2019
0960-8524/

and other gaseous pollutants under sunlight, thereby producing severe secondary pollution problems, e.g., photochemical smog and ozone (Shen and Zhang, 2019; Zhang et al., 2017). Therefore, safe, environmentally friendly, and efficient techniques that can be used to remove VOCs and to meet the strict emission standards are necessary. VOC levels in the range 0.5–15 mg m^{-3} are considered acceptable in China. Examples of efficient treatments include adsorption, photodegradation, bio-purification, and non-thermal plasma (NTP). Each technology has its own application, advantages, and disadvantages. Adsorption is a promising option for the removal of low-concentration VOCs at room temperature and atmospheric pressure (Shafiei et al., 2018).

Adsorption is a facile recycling technique with easy application. It has been widely used to remove and recover VOCs, especially some recyclable materials, from polluted air. Activated carbon (AC) is the most common adsorbent because of its large surface area and good pore volume (Yu et al., 2019). However, commercialized AC has disadvantages, such as flammability, no resistance to humidity, and high regeneration cost. Therefore, several inexpensive and effective alternative materials (rice straw, barley straw, and sugarcane bagasse) with low adsorption capacities are used as adsorbents (Aksu, 2005). Through physical and chemical modification that change the structural characteristics of these adsorbents, their adsorption capacities are improved. Recently, biosorbents have attracted much attention from researchers. Several common microorganisms, such as bacteria, fungi, yeast, and algae, are used as biosorbents and have special surface properties (e.g., adhesion and flocculation abilities), which enable them to adsorb various pollutants from the surroundings (Vijayaraghavan and Yun, 2008). For example, dead *Bacillus subtilis* has good adsorption properties for cationic basic dyes (Kim et al., 2015). Aksu and Tezer (2000) found that dead *Rhizopus arrhizus* could adsorb Remazol Black B dye, and this adsorption was due to the interaction between the cellular components of microorganisms (such as lipids/polysaccharides) and dye anions (such as azo-based chromophores) (Aksu and Tezer, 2000).

Biosorbents are cost effective because of the abundant sources and moderate preparation conditions. Several studies showed that the wastes from most industrial processes (e.g., fermentation and waste water treatment) that contain abundant microorganisms can be used as biosorbents, most of which perform better than AC. Compared with the living biomass, dead biomass is more convenient for adsorption, because the toxicity of adsorbate and continuous nutrition provision should not be considered during the process (Dhankhar and Hooda, 2011). In addition, dead biomass is easily recycled and regenerated and adsorbs more pollutants than living biomass (Aksu, 2005; Crini, 2006; Vijayaraghavan and Yun, 2008). Wang et al. (2017) compared the adsorption performance of live and dead yeast to the uranium ions and found that the dead yeast could reach the adsorption equilibrium state in 300 min with an adsorption efficiency of 85%, which was higher than that of live yeast (adsorption efficiency of 70% in 300 min). Luo et al. (2014) studied the adsorption of high molecular weight polycyclic aromatic hydrocarbons by live and dead microalgae, and the results showed that the adsorption capacity of dead algal cells was four times higher than that of live algal cells (Luo et al., 2014).

The adsorption properties of biosorbents depend on their structural characteristics, e.g., pore distribution, specific surface area, and functional groups (Ramrakhiani et al., 2011). Such modifications could lead to excellent adsorption capacity of biosorbents. Common chemical modification includes the introduction (oxidation, amino reduction, and phosphorylation) or hiding (decarboxylation and deamination) of functional groups, hydrolysis treatment (acids hydrolysis and bases hydrolysis), and high-energy radiation (using γ-irradiation, microwave radiation, and electro-magnetic radiation) (Park et al., 2010). The adjustment of surface functional groups is more effective than other changes. By introducing certain functional groups such as amino and carboxyl groups onto the cell surface, the number of effective adsorption binding sites increases. Thus, a larger adsorption capacity can be obtained. Huang et al. (2016) used cetyl trimethyl ammonium bromide-modified *Aspergillus versicolor* biomass to introduce more amino and amide groups. The adsorption performance of reactive black 5 increased by 4.4 times (Huang et al., 2016). Specific surface area is another important characteristic of the adsorbent that influences adsorption capacity (Cheng et al., 2019). Compared with bacteria, fungi have better surface characteristics, i.e., larger specific surface area and more adsorption sites, thereby making them more suitable for adsorbing hydrophobic VOCs. Cheng et al. (2019) found that the adsorption capacity of fungi on gaseous n-hexane and ethyl acetate was 4.38 and 4.11 times than that of bacteria, respectively, because a large specific surface area of the fungus leads to an increase in the number of hydrophobic regions on its surface area (Cheng et al., 2019). Microbial biosorbents are currently used to remove metals and organic pollutants from wastewater. Therefore, the microbial biomass can possibly be used as adsorbent to remove VOCs from waste gas.

In the present study, some novel microbial adsorbents were synthesized using the selected fungal (*Ophiostoma stenoceras* LLC) or bacterial (*Pseudomonas veronii* ZW) cells, and the adsorption capacity was enhanced through chemical modification. The biosorption performances of VOCs, i.e., ethyl acetate, alpha(α)-pinene, and n-hexane, by the original and chemically modified bacterial or fungal biosorbents were compared, including the adsorption capacity, adsorption kinetics, and adsorption mechanism. In addition, their surface characteristics, e.g., specific surface area, functional group, and chemical composition, were analyzed by Brunauer-Emmett-Teller (BET), Fourier-transform infrared spectroscopy (FTIR), and X-ray photoelectron spectroscopy (XPS). Such results from the current study suggested that the synthesized biosorbents, especially the fungal biosorbent, are promising adsorbents for VOC removal.

2. Materials and methods

2.1. Preparation of biosorbents

2.1.1. Materials

One strain of fungus, *O. stenoceras* LLC (CCTCC NO. M 2014531), and one strain of bacterium, *P. veronii* ZW (CCTCC NO. M 29313), which were isolated by our groups, were selected as typical microorganisms. Both can biodegrade α-pinene and grow with α-pinene as the sole carbon source.

All the chemical reagents used in the present study were of analytical grade.

2.1.2. Unmodified biosorbent preparation

The strain *Pseudomonas* ZW and *Ophiostoma* LLC were enriched in sterilized (394 K, 20 min) Luria-Bertani (LB) medium and potato dextrose agar (PDA) medium, respectively. After centrifugation, the microbial cells were lyophilized to remove water using a vacuum freezing dryer LGJ-10 (Songyuanhuaxing Tech. Co., Ltd., Beijing, China), under the following conditions. First, the freezing temperature was maintained at 193 K for 2 h. Then, the temperature increased to 258 K, which was kept for 14 h, and then further increased to 283 K, which was kept for 10 h. More than 90% water was sublimated. Next, the temperature was increased to 293 K, and the residual water was evaporated immediately (Cheng et al., 2019). The obtained lyophilized cells were named as original fungal (O-F) biosorbent and original bacterial (O-B) biosorbent, respectively. Both were stored for further use.

2.1.3. Chemical modification of the lyophilized biomass

Three chemical modifications were used, namely, carboxyl esterification, base hydrolysis, and aminomethylation. After chemical modification, the obtained biosorbents (C-F, B-F, and A-F) were referred to the O-F's modification by carboxyl esterification, base hydrolysis, and aminomethylation treatment. Similarly, A-B was referred to

biosorbent O-B, which was modified by aminomethylation.

Specifically, 1.0 g lyophilized biomass of strain LLC and ZW were suspended in 100 mL of 99.9% acidic methanol solution and 1 mL of hydrochloric acid (12 mol/L HCl), respectively. The suspension was continuously stirred at 60 °C for 48 h and then cooled to room temperature. The cells were then washed three times with double distilled (DD) water to quench the esterification reaction. Afterward, the obtained materials were lyophilized again to obtain the absorbents. The chemical esterification reaction is shown as follows, where R represents all of the components in the dead cells (Fang et al., 2011):

$$RCOOH + CH_3OH \xrightarrow{H^+} RCOOCH_3 + H_2O$$

To increase the availability of carboxyl groups that may be better for VOC adsorption, base hydrolysis was carried out. Lyophilized biomass at 1 g was reacted with 35 mL of 0.1 mol L^{-1} NaOH for 2 h to perform the following reaction (Fang et al., 2011):

$$RCOOCH_3 + NaOH \rightarrow RCOO^- + CH_3OH + Na^+$$

The third modification could introduce the amino group to the cell surface through the methylation process. Raw biomass at 1 g was mixed with 20 mL of formaldehyde (HCHO) and 40 mL of formic acid (HCOOH), and then, the mixture was shaken on a rotary shaker for 6 h at 125 rpm during which the following reaction took place (Park et al., 2005):

$$RCH_2NH_2 \xrightarrow{HCHO+HCOOH} RCH_2N(CH_3)_2 + CO_2 + H_2O$$

After the reaction, the suspension was centrifuged, and the supernatant was discarded. The centrifugal precipitate was washed three times with DD water, centrifuged, and then lyophilized.

2.2. Adsorption research

2.2.1. Adsorbates

Three common substances, namely, α-pinene, n-hexane, and ethyl acetate, were selected as the adsorbates. Their Henry coefficients (H), which are different from each other, represent three kinds of substances with different hydrophobicity values, namely, weak, moderate, and strong.

2.2.2. Adsorption performance

The unmodified or modified biosorbent at 0.10 g was added to shake flasks, and one of the selected organic compounds (α-pinene, n-hexane, or ethyl acetate at a final concentration of 15 mg·m^{-3}) was added to each shake flask. The shake flask was sealed by a Teflon stopper and then twined by a high temperature resistant aluminum foil. All the sealed shake flasks were shaken at 303 K, and the concentration of the organic compound in the gas phase was measured at 0, 30, 60, 90, 120, 240, and 480 min. The shake flask with no biosorbent was used as the blank control, and results showed there was no leaks during the evaporation of the solvent. The adsorption uptake of VOC vapor on the biosorbents was calculated according to the following equations:

$$R = \frac{C_0 - C_t}{C_0} \times 100\% \quad (1)$$

$$q = \frac{(C_0 - C_t) \times V}{m} \quad (2)$$

where R is the adsorption efficiency (%), C_0 is the VOC concentration (mg·m^{-3}) before adsorption, C_t is the VOC concentration (mg·m^{-3}) after adsorption t, q is the adsorbed amount per gram biosorbent (mg·g^{-1}), V is the shake flask volume (m^3), and m is the adsorbent mass (g). All experiments were conducted at constant temperature.

To obtain the equilibrium adsorption amount q_e (mg·g^{-1}) and the equilibrium concentration C_e (mg·m^{-3}), the adsorption isotherms of the synthesized biosorbents (unmodified or modified) for each hydrophobic VOC were described by Langmuir and Freundlich adsorption equilibrium isotherms (at 303 K), which are expressed as follows (Cheng et al., 2019):

$$\frac{1}{q_e} = \frac{1}{q_{max}} + \frac{1}{K_L \hat{A} \cdot q_{max} \hat{A} \cdot C_e} \quad (3)$$

$$\ln q_e = \ln K_F + \frac{1}{n} \ln C_e \quad (4)$$

where q_e is the equilibrium adsorption amount (mg·g^{-1}), q_{max} is the maximum adsorption amount (mg·g^{-1}), C_e is the equilibrium concentration (mg·m^{-3}), K_L (m^3·mg^{-1}) and K_F ((m^3)$^{1/n}$·$mg^{(1-1/n)}$·g^{-1}) are the adsorption constants, and n is a constant related to temperature.

The adsorption kinetic model is useful for determining whether physical or chemical adsorption of VOCs takes place (Zou et al., 2019). The kinetic analysis of these synthesized biosorbents was carried out by using three kinetic models, namely, the pseudo-first-order, pseudo-second-order, and intra-particle diffusion models, as follows (Song et al., 2016):

$$\ln(q_e - q_t) = \ln q_e - k_1 t \quad (5)$$

$$\frac{t}{q_t} = \frac{t}{q_e} + \frac{1}{k_2 q_e^2} \quad (6)$$

$$q_{t=k_i t^{0.5}} \quad (7)$$

where q_e and q_t (mg·g^{-1}) are the amount of VOCs adsorbed at equilibrium state and at time t, respectively; k_1 (min^{-1}) is a rate constant of the pseudo-first-order adsorption; k_2 (g·mg^{-1} min) is a rate constant of the pseudo-second order adsorption; and k_i (mg·g^{-1} $min^{0.5}$) is an intra-particle diffusion rate constant.

The validity of these models was evaluated by the coefficient of regression, R^2, which varies between 0 and 1, and by the normalized standard deviation Δq (%), which is defined as follows (Song et al., 2016):

$$\Delta q = 100 \sqrt{\frac{\sum \left(\frac{q_{exp} - q_{mod}}{q_{exp}} \right)^2}{N - 1}} \quad (8)$$

where q_{exp} and q_{mod} are the adsorption capacities obtained from isotherm experiments and models, respectively, and N is the number of adsorption isotherm data points.

2.3. Analytical methods

Gaseous concentrations of the three selected organic compounds were determined by a 6890 gas chromatograph (Agilent Technologies, Palo Alto, CA, USA) equipped with an HP-Innowax column (30 m × 0.32 mm × 0.5 μm). Gaseous samples at 800 μL were collected from the sealed bottle by an airtight syringe and then analyzed under the following temperature conditions: injector 483 K, oven 363 K, and detector 473 K for α-pinene and ethyl acetate; injector 523 K, oven 353 K, and detector 573 K for n-hexane.

XPS analysis was conducted on an ESCALAB 250Xi model (Thermo Fisher Scientific, CA, USA) with an Al Kα X-ray ($h\nu$ = 1486.6 eV) radiation excitation source. The pore structures of the synthesized biosorbents were determined by N_2 adsorption using a sorption analyzer (ASAP 2020, Micromeritics Co., GA, USA) at 77 K. The surface functional groups were analyzed by a FTIR (Nicolet 6700, 186 Thermo Scientific Co., USA). Contact angle measurements were conducted on an optical contact angle goniometer (OCA20, Data Physics Instruments Co., Germany) at room temperature.

2.4. Statistical analysis

All experiments were repeated at least three times. Data were statistically analyzed by ANOVA using SPSS software package (IBM SPSS statistic 20.0). The least significant difference (LSD) test was used to

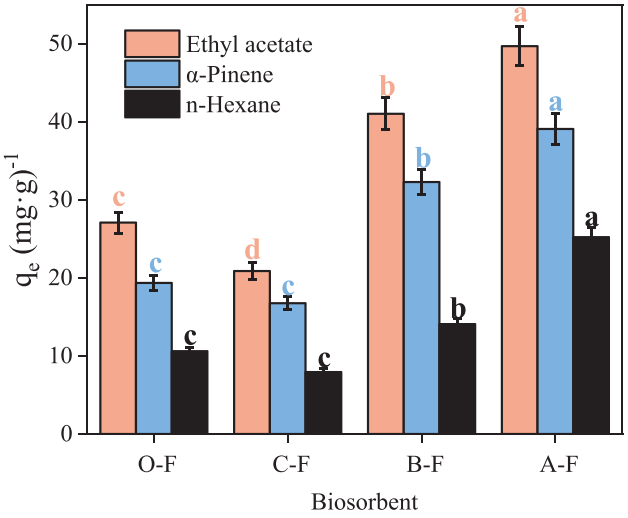

Fig. 1. Adsorption capacities of VOCs by unmodified and chemical-modified fungal biosorbents at 303 K. Means and their standard errors are presented (n = 3). Statistically different means are indicated with different letters (P < 0.05, ANOVA, LSD test).

analyze the statistical significance of differences about the data. The differences were significant at p < 0.05.

3. Results and discussion

3.1. Comparison of modification effects

Most biosorbents had different adsorption capacity to these selected compounds. Through the calculation of adsorption capacity per unit mass of sorbent, A-F was shown to have the best adsorption performance, followed by B-F and C-F (Fig. 1). The adsorption uptake values for A-F were 49.68 mg·g^{-1} (ethyl acetate), 39.07 mg·g^{-1} (α-pinene), and 25.22 mg·g^{-1} (n-hexane), which were 1.83, 2.01, and 2.40 times higher than the values for biosorbent O-F, respectively. As shown in Fig. 1, the adsorption capacity of weak hydrophobic compounds (e.g., ethyl acetate) by these synthesized biosorbents was larger than that of the strong hydrophobic compounds (e.g., n-hexane). The surface of these biosorbents was weakly hydrophobic, as revealed by XPS and contact angle analysis. Weak hydrophobic compounds tended to be adsorbed by these biosorbents (named as similar miscibility) (Sugimoto et al., 2007).

Several studies showed that carboxyl esterification decreased the carboxyl group on the surface. Base hydrolysis led to the serious decomposition of cell structure (such as breakage of cellulose polymer), whereas aminomethylation reduced the HN– groups and increased the CH_3– group on the surface. All these changes were or were not conducive to adsorption (Fang et al., 2011; Wang et al., 2011). The aminomethylation was the best chemical modification. In addition, the obtained biosorbents had good VOC adsorption performance. Aminomethylation introduces the CH_3– groups to the biosorbent's surface, thereby resulting in good VOC adsorption performance. Based on the above-mentioned results, aminomethylation was used to modify the bacterial strain ZW.

O-B's capacity to adsorb ethyl acetate, α-pinene, and n-hexane were 12.75, 8.56, and 5.56 mg·g^{-1}, which were lower than that of O-F biosorbents (27.08, 19.35, and 10.61 mg·g^{-1}, respectively). The results were the same as those reported in the literature, because the specific surface area of the fungi was larger than that of the bacteria (Cheng et al., 2019).

Compared with the O-B biosorbents, the adsorption efficiency (% removal) and adsorption capacity of A-B were 13.34% and 36.02 mg·g^{-1} (ethyl acetate), 10.26% and 26.17 mg·g^{-1} (α-pinene), and 7.54% and 14.81 mg·g^{-1} (n-hexane). Aminomethylation modification was conducive to the adsorption of VOCs by the biosorbents sourced from strain ZW. Based on the above results, the aminomethylation modification was effective for the fungal and bacterial materials. Therefore, the following studies focused on the fungal and bacterial biosorbents modified by aminomethylation.

3.2. Surface characteristics of biosorbents

3.2.1. BET analysis

Specific surface area is an important factor affecting the ability of biosorbents to adsorb target compounds. The isotherms of these four biosorbents could be classified as type-IV isotherms characterized by H3-type hysteresis loop according to the IUPAC (El-Shafey et al., 2016) (Fig. 2a, b, c, and d). The appearance of hysteresis loop could be attributed to the capillary condensation of N_2 in the pores (Zhang et al., 2016a). In addition, the amount of nitrogen in the biosorbents increased sharply at high relative pressure (P/P_0 > 0.95), thereby indicating that some macropores were present. In the low-pressure zone, the adsorption-desorption curve was not closed, probably due to the presence of micropores on the adsorbent surface. Based on these analyses, micropores, mesopores, and macropores existed in the synthesized adsorbents. The pore size distribution was calculated by the Barrett–Joyner–Halenda (BJH) model as shown in Fig. 2e, f, g, and h. The most probable pore diameters of O-B, A-B, O-F, and A-F biosorbents were 3.01, 2.50, 2.79, and 2.02 nm, respectively. All biosorbents had diameters in the range of 2–50 nm, indicating that the mesoporous material dominated their pore structures. Using the BET method, the specific surface area of the bacterial biosorbent increased from 11.52 m^2·g^{-1} to 13.70 m^2·g^{-1}, whereas the specific surface area of the fungal biosorbent increased from 15.69 m^2·g^{-1} to 20.38 m^2·g^{-1}. Such increase was due to the grafting of the CH_3– group on the surface after aminomethylation modification, which enriched the pore structure and increased the specific surface area (Bai and Abraham, 2002). Furthermore, this increase was more favorable for the adsorption performance of the biosorbent. The specific surface area of fungal biosorbents was significantly higher than that of bacterial biosorbents, which was consistent with the adsorption performance of VOCs in the present study.

Some studies showed that when the ratio of the adsorbent pore size to the molecular dynamic diameter of the adsorbate is approximately three times, the adsorption performance might be better (Cheng et al., 2019). In the present study, the kinetic diameters of ethyl acetate, α-pinene, and n-hexane were 0.67, 0.70, and 0.49 nm, respectively. The main pore diameter of the A-F biosorbent (2.02 nm) was much closer to approximately three times of the molecular dynamic diameters of these compounds. As a result, the adsorption capacity of A-F for these VOCs was the largest among the synthesized biosorbents.

3.2.2. FTIR analysis

Some peaks were at 1641 cm^{-1} (C═C and C═O vibration), 1532 cm^{-1} (C–N and N═O vibration), 1238 cm^{-1} (–COO– vibration), and 1058 cm^{-1} (C–O–C and –OH vibration) (Yee et al., 2004; Yun et al., 2001), which were attributed to amide I, amide II, carboxypolysaccharide, and polysaccharide, respectively. In addition, the wide and strong frequency bands between 3000 and 3660 cm^{-1} were attributed to the overlapping of O–H and N–H tensile vibrations (Ashkenazy et al., 1997).

The positions and numbers of the absorption peaks in the FTIR spectrum were the same, suggesting that the aminomethylation did not cause significant structural changes on the surface of the modified biosorbents (Chen et al., 2010). Related studies showed that the difference in the functional groups affected the adsorption of biosorbents to organic compounds (Aksu, 2005). Daneshvar et al. (2017) studied the adsorption of modified algae on three kinds of dyes and confirmed that some functional groups affected the biosorption process. For example, a high amount of COOH and COO– groups distributed on the

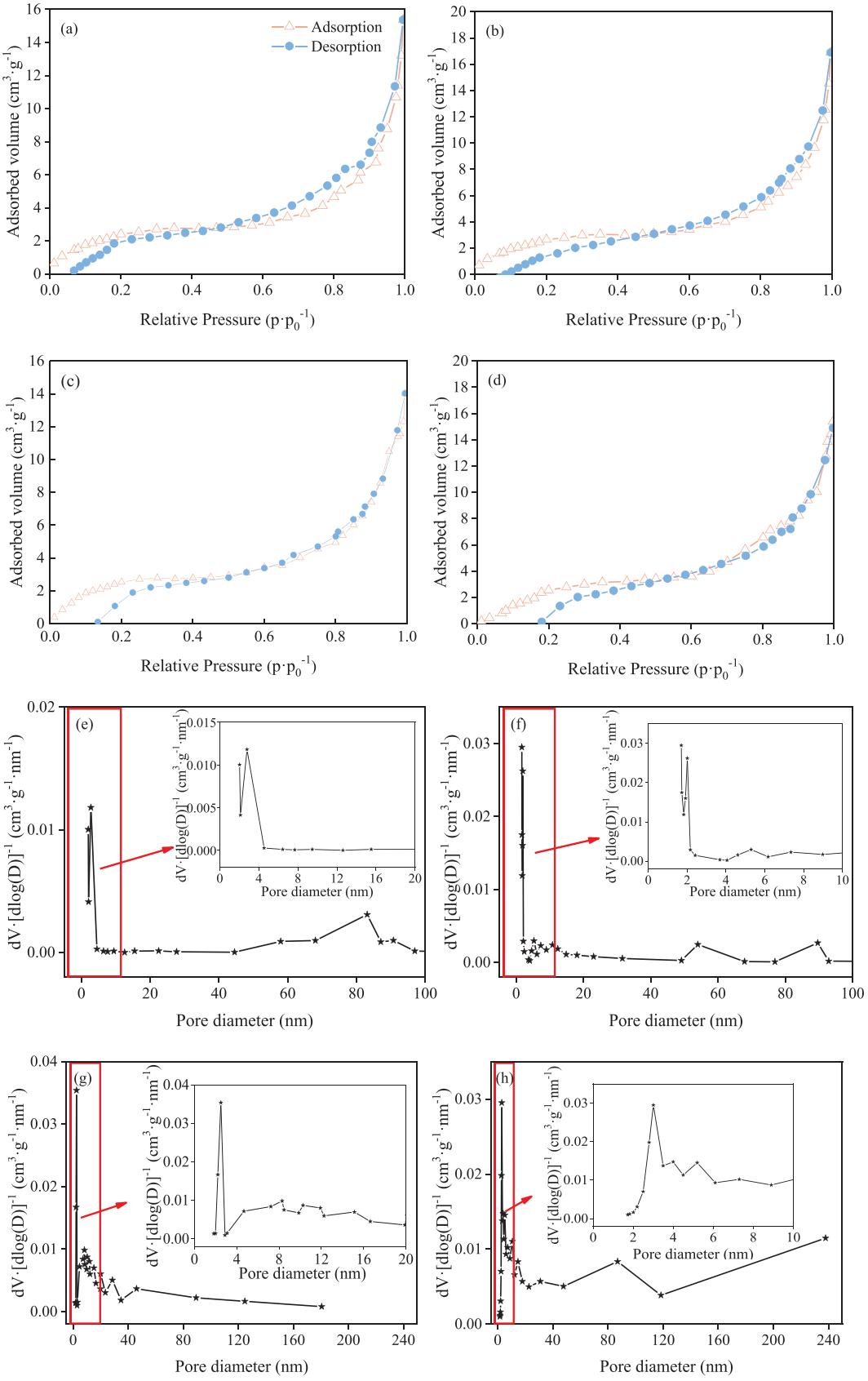

Fig. 2. N_2 adsorption–desorption curves of (a) O-F, (b) A-F, (c) O-B and (d) A-B; pore size distribution of (e) O-F, (f) A-F, (g) O-B and (h) A-B.

surface enhanced the adsorption efficiency of cationic dyes, from 42.50% to 62.00% (Daneshvar et al., 2017). Aminomethylation is a valuable method of blocking the amine groups distributed on the surface of biosorbents by methylation (Das et al., 2008). In the present study, the absorption peak of the A-F and A-B biosorbents near 1380 cm^{-1} was enhanced and sharpened compared with those of the O-F and O-B biosorbents, because the methyl group ($-CH_3$) introduced during the methylation replaced H, which was in the amino group (Yee et al., 2004). A high number of methyl groups may help the biosorbents adsorb VOCs. Similarly, the absorption peak near 1238 cm^{-1} was enhanced, which was related to the vibration of the polysaccharide. Notably, the amino group is a hydrophilic group, whereas the methyl group is a hydrophobic group (Gu et al., 2017; Zhang et al., 2017). A high number of methyl groups results in a highly hydrophobic surface, which was beneficial to the adsorption capacity of the biosorbent. Compared with unmodified biosorbents (O-B and O-F), the modified biosorbents (A-B and A-F) showed a significant decrease in the peak intensity near 3100–3660 cm^{-1}, which indicated that the O−H and N−H groups remarkably decreased. This decrease in peak intensity might cause low hydrophilicity, which would make the surface more favorable to the adsorption of hydrophobic VOCs (Qiu et al., 2018; Zhang et al., 2017).

3.2.3. Contact angle analysis

Measurement of contact angle was carried out to evaluate the hydrophilicity of the synthesized biosorbents before and after aminomethylation. If the water contact angle is greater than 90°, then the surface is classified as hydrophobic, and if it is less than 90°, then the surface is hydrophilic (Wang et al., 2011). The water contact angles of O-B, A-B, O-F, and A-F were 48°, 98°, 31°, and 75°, respectively. The contact angle increased after modification, thereby suggesting that the modified surface tended to be more hydrophobic (Li et al., 2016). High hydrophobicity might be related to the decrease in the hydrophilic groups (e.g., the hydroxyl and carboxyl groups) (Qiu et al., 2018). After aminomethylation (the hiding of amino and hydroxyl groups), the hydrophobicity of these synthesized biosorbents increased, which benefitted the adsorption of VOCs (Liu et al., 2016). Contact angle measurements were consistent with the results from the previous FTIR analysis.

3.2.4. XPS analysis

The chemical compositions and alterations of the biosorbent surface before and after modification were analyzed by XPS. The synthesized materials were similar to many other biomass carbon materials that contained C, O, and N elements. The high-resolution spectra of C1s, O1s, and N1s of the synthesized biosorbents show that each sample had 3, 2, and 2 constituents of C1s, O1s, and N1s, respectively, but with different intensities. The elemental composition, the binding energy, and the corresponding assignments are shown in Tables 1 and 2. The surface of modified biosorbents contained relatively abundant groups,

Table 1
Binding energy, assignments, and quantification of XPS spectral bands for surface composition of modified and unmodified biosorbents.

Element	Peak (eV)	Percentage (%)				Assignment
		O-F	A-F	O-B	A-B	
C1s	284.8	40.11	48.93	43.96	50.60	C−(C or H)
	286 (286.2)	17.07	14.04	20.56	16.98	C−(O or N) C−(O or N)
	287.86	12.43	11.47	7.45	8.09	C═O, OCO−
N1s	399.9	4.30	1.30	4.95	2.07	Nonprotonated N
	401.5	1.24	0.91	0.75	0.55	Protonated N (Graphitic N)
O1s	531	5.10	5.58	8.301	7.98	C═O, P═O
	532.5	19.76	17.77	14.03	13.73	C−OH, C−O−C, P-OH,

Table 2
Proportions of carbon atomic concentrations with each molecular constituent and predominant constituent for modified and unmodified biosorbents.

Element	O-B	A-B	O-F	A-F
Total C	71.97	75.67	69.60	74.44
Total O	22.34	21.71	24.85	23.35
Total N	5.69	2.62	5.55	2.21
C_{PR}	0.28	0.12	0.29	0.11
C_{PS}	0.26	0.30	0.32	0.33
C_{HC}	0.46	0.58	0.39	0.56
PR%	32.29	14.57	32.14	13.13
PS%	35.15	42.68	41.56	46.18
HC%	32.56	42.75	26.30	40.69

which was consistent with the results of the FTIR analysis.

The C1s XPS spectrum was curved-fitted into three peaks with binding energies at 248.8, 286.0 (286.2), and 287.86 eV that corresponded to the C− (C or H; attributed to lipid), C− (O or N; attributed to alcohol, amine, or amide), and C═O or OCO− (attributed to hemiacetal, acetal, amide, and carboxylate) groups, respectively (Cheng et al., 2019). According to the N1s spectra, two peaks at 399.9 and 401.5 eV were present, which correspond to nonprotonated nitrogen (typical of amide and amine) and protonated nitrogen (typical of ammonium or protonated amine), respectively. In the O1s deconvolution spectra, the peak was broken down into two components (at 531.0 and 532.5 eV). These two components referred to the C−O or C═O (attributed to carboxyl, carbonyl, ester, or amide) and C−OH, C−O−C, or P−OH (attributed to alcohols, acetals, or hemiacetal) groups (Cheng et al., 2019). The XPS results indicated that various functional groups, such as carbonyl, carboxyl, amide, and phosphoryl, were distributed on the surface of these biosorbents, which were important for the biosorption of metals and organic compounds (Zhang et al., 2016b). In addition, after modification, the content of nonprotonated nitrogen was remarkably reduced, and its amount in fungal biosorbents (O-F and A-F) was lower than that in bacterial biosorbents (O-B and A-B), thereby indicating that the modification successfully reduced the amount of amino group in the biosorbents.

As shown in Table 1, the proportion of C, O, and N elements on the surface changed after aminomethylation. The relative C/N content of fungal biosorbent increased (from 12.56 to 33.68). Likewise, this value for bacterial biosorbent also increased (from 12.63 to 28.88). The reason for the increase in C/N content might be that the H in the amino groups was replaced by H in the methyl groups during aminomethylation.

The surface components of microbial cells are polysaccharides (PS), proteins (PR), and lipid compounds (hydrocarbon-like compounds, HCs). Their amounts are calculated by using the following formula: $C_{PR} = 3.584$ (N/C); $C_{PS} = 1.20$ ((O/C) – 0.325 C_{PR}); and $C_{HC} = 1 - C_{PS} - C_{PR}$ (Cheng et al., 2019). As shown in Table 2, after modification, the proportion of hydrocarbon compounds and polysaccharides of A-F or A-B biosorbents increased (from 26.30% to 40.69% and 41.56% to 46.18% or from 32.56% to 42.75% and 35.15% to 42.68%, respectively), whereas the proportion of protein in A-B and A-F biosorbents decreased. Based on these values, the amount of surface components changed after modification. The increased in the amount of hydrocarbon and polysaccharide compounds magnified the change in the hydrophobic region, which was more suitable for the adsorption of hydrophobic organic compounds (Cheng et al., 2019; Sheng et al., 2010).

3.3. Adsorption characteristics

3.3.1. Adsorption isotherms

Synthesized biosorbents weighing 0.1 g and organic compound concentrations ranging from 15 $mg{\cdot}m^{-3}$ to 180 $mg{\cdot}m^{-3}$ were utilized

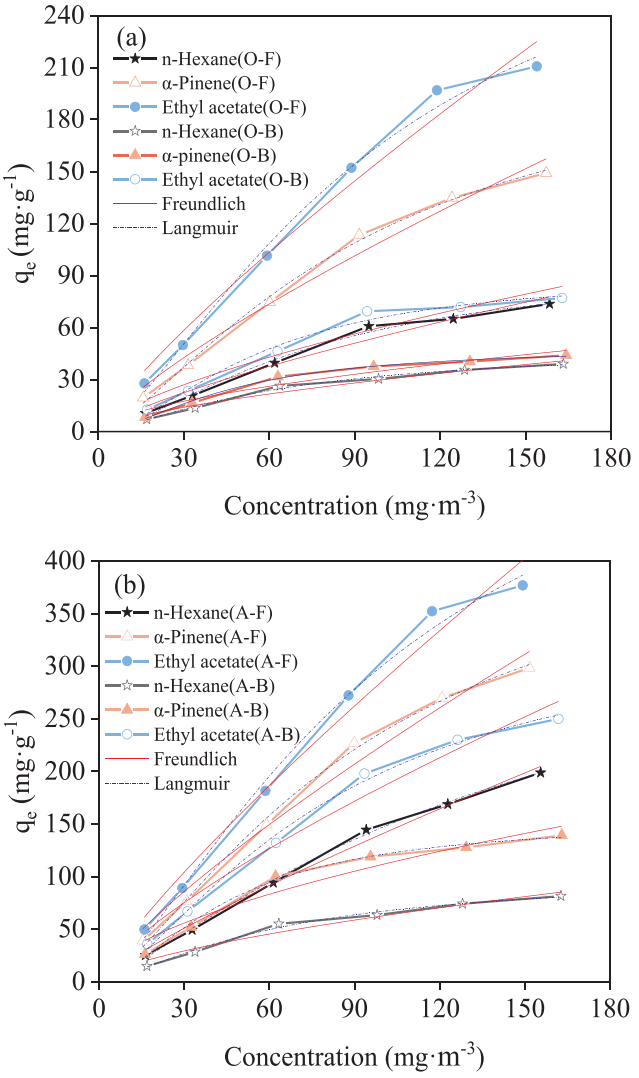

Fig. 3. Adsorption isotherms for different synthesized biosorbents: (a) O-F or O-B and (b) A-F or A-B.

Table 3
Langmuir and Freundlich kinetic constants for different biosorbents.

Biosorbent	VOC sample	Langmuir			Freundlich		
		R^2	K_L	q_{max}	R^2	K_F	n
O-F	n-Hexane	0.9885	0.0014	97.9705	0.9607	1.7687	1.3389
	α-Pinene	0.9954	0.0015	220.7941	0.9803	2.9133	1.2679
	Ethyl acetate	0.9936	0.0013	331.3812	0.9925	3.5304	1.2122
O-B	n-Hexane	0.9920	0.0030	43.4951	0.9639	1.6342	1.5836
	α-Pinene	0.9920	0.0017	48.7539	0.9397	2.4539	1.7309
	Ethyl acetate	0.9876	0.0001	91.1358	0.9222	2.7733	1.4946
A-F	n-Hexane	0.9974	0.0019	372.7025	0.9890	2.8675	1.3030
	α-Pinene	0.9974	0.0017	454.4450	0.9823	5.6345	1.2490
	Ethyl acetate	0.9904	0.0015	620.3632	0.9765	5.9779	1.1903
A-B	n-Hexane	0.9866	0.0031	101.1716	0.9636	3.4371	1.5860
	α-Pinene	0.9919	0.0018	153.9045	0.9390	7.8951	1.7385
	Ethyl acetate	0.9933	0.0015	343.8049	0.9648	5.8406	1.3313

for each organic compound. The adsorption isotherm curves are shown in Fig. 3, whereas the obtained model parameters and R^2 values are listed in Table 3.

The adsorption capacities of the synthesized biosorbents were found to be in the following order: A-F > A-B ≈ O-F > O-B. All models were consistent with the experimental results according to the correlation coefficient R^2 (the consistency between the experimental data and the predicted values of the model), which was larger than 0.90 (Table 3). Moreover, compared with the Freundlich model, the Langmuir model was found to be more suitable for the description of the adsorption process, in which the isothermal adsorption of VOCs by these biosorbents was a monolayer adsorption process, and the adsorption was governed by electrostatic attraction (Zhang et al., 2019b). The Freundlich model has an n value greater than 1, which indicates that the adsorption of VOCs by these biosorbents was favorable (Wang et al., 2019). The parameter n characterized the following adsorption processes between the adsorbent and the adsorbate: physical ($n > 1$), chemical ($n < 1$), or linear ($n = 1$) (Zou et al., 2019). In the current study, the parameter n was greater than 1, thereby suggesting that the adsorption of VOCs by these biosorbents was physical.

There was a relationship between q_{max} and the hydrophobicity of selected VOCs. Referring to the adsorption capacity of the adsorbate, its adsorption performance was positively correlated with the hydrophobicity of the surface functional groups of the adsorbent (Liu et al., 2016). In the present study, three VOCs with different hydrophobicity values (ethyl acetate, α-pinene, and n-hexane) were chosen. After aminomethylation, the adsorption capacities of A-F increased by 3.80, 2.06, and 1.89 times in n-hexane, α-pinene, and ethyl acetate, respectively, and these values were higher than those of unmodified O-F. Aminomethylation could increase surface hydrophobicity, which enables easy adsorption of hydrophobic compounds. The similarity of hydrophobicity between the adsorbent surface and VOCs was very important for adsorption (Liu et al., 2016).

3.3.2. Adsorption kinetics

As shown in Fig. 4, for each biosorbent, VOC sorption capacity increased rapidly in the first 30 min, then rose slowly, and finally reached the equilibrium state at 150 min. These variations were due to the fact that the empty surface sites were not occupied and the adsorption rate was relatively fast at the beginning. With these positions being occupied by adsorbates, the adsorption rate decreased gradually until the final adsorption-desorption equilibrium was reached (Wang et al., 2019).

Table 4 presents the parameters of these three models for n-hexane, α-pinene, and ethyl acetate adsorption. A high R^2 value indicated that the model could describe these adsorption processes. Furthermore, R^2 of the pseudo-first-order kinetic model was the highest, and the calculated value q_e was very close to the experimental value. The other two models with low R^2 values suggested that they might not be suitable in describing the adsorption of VOCs by these synthesized biosorbents. Table 4 shows that the normalized standard deviation of pseudo-first order model was smaller than that of the pseudo-second order model, which was consistent with the fitting results shown in Fig. 4. Therefore, the pseudo-first-order models are more suitable for predicting the VOCs adsorption by these biosorbents. Several studies showed that if the pseudo-first order model provided better fit result, then the adsorption was a physical process; while the pseudo-second order model fits better, then it was chemical adsorption (Song et al., 2016). Based on these fitting values, the adsorption of VOCs by these biosorbents was mainly a physical adsorption (pseudo-first-order) while chemical adsorption (pseudo-second-order) probably took place at a smaller proportion (Ammendola et al., 2017; Chen et al., 2018). The R^2 values for intra-particle diffusion model were lower (almost 0.70). Thus, the adsorption on the outer surface was the main mechanism, whereas the diffusion within the particles was the second mechanism and was less preferable to occur (Wang et al., 2019).

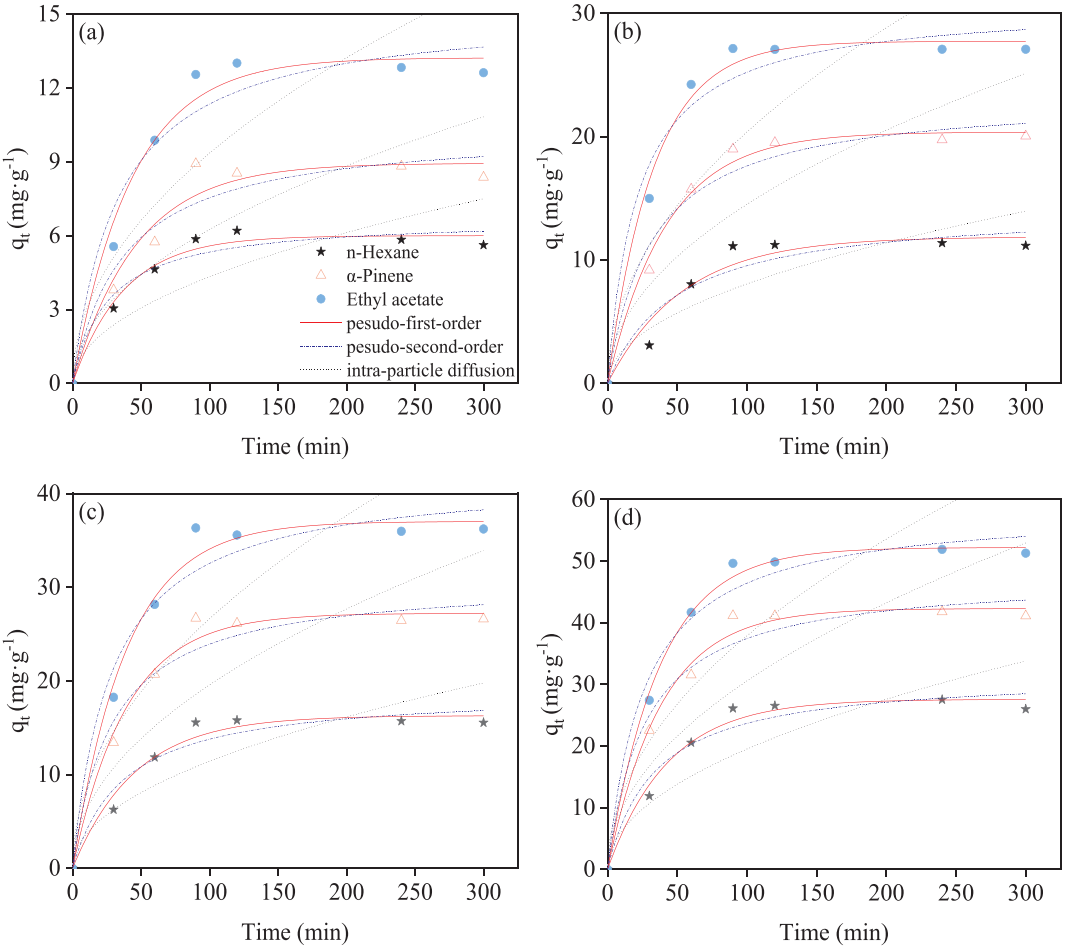

Fig. 4. Adsorption kinetic model of VOCs by different biosorbents at 303 K: (a) O-B, (b) O-F, (c) A-B, (d) A-F.

3.4. Effect of temperature variation on the adsorption capacity of VOCs

To explore the adsorption capacity and behavior of O-F and A-F biosorbents at different adsorption temperatures, the capacity for VOC adsorption at several different temperatures (293, 303, 313, 323, and 333 K) and atmospheric pressure was measured. With increasing adsorption temperature, the adsorption amount of VOCs decreased rapidly before 313 K, and began to decrease slowly after 313 K. The O-F and A-F biosorbents were very sensitive to temperature, indicating the process is exothermic (Bhatnagar et al., 2010). For example, when the temperature was 293 K, the adsorption capacities of ethyl acetate, α-pinene, and n-hexane by A-F biosorbent were 68.95, 57.09, and 39.09 mg g^{-1}, respectively. As the adsorption temperature increased to 333 K, these values decreased to 15.64, 7.95, and 3.56 mg g^{-1}, respectively. The adsorption capacity of VOCs decreased when the adsorption process temperature increased, thereby indicating that the adsorption mode between the synthesized biosorbents and VOCs is physisorption (Ahmed and Jhung, 2015). This conclusion was similar to that obtained through adsorption kinetic analysis. The adsorption quantity of ethyl acetate by the O-F biosorbent decreased with

Table 4
Constants of three adsorption kinetic models for VOCs by different biosorbents at 303 K.

Biosorbent	VOC sample	q_e (exp)*	Pseudo-first-order kinetic model				Pseudo-second-order kinetic model				Intraparticle diffusion model		
			R^2	q_e (mod)*	K_1	Δq (%)	R^2	q_e (mod)	K_2	Δq (%)	R^2	k_{int}	C
O-F	n-Hexane	10.1858	0.9448	11.8716	0.0185	0.2739	0.9098	14.2836	0.0014	1.6184	0.7358	0.6965	1.3844
	α-Pinene	19.5279	0.9892	20.3750	0.0237	0.0188	0.9619	23.3624	0.0013	0.3856	0.7569	1.1455	3.8678
	Ethyl acetate	27.7712	0.9891	27.7315	0.0301	0.0002	0.9598	30.7982	0.0015	0.1188	0.6731	1.4894	6.9432
O-B	n-Hexane	5.5605	0.9753	5.9994	0.0267	0.0623	0.9379	6.7171	0.0058	0.4326	0.6706	0.3238	1.3829
	α-Pinene	8.2735	0.9520	8.9413	0.0214	0.0065	0.9166	10.3656	0.0026	0.6393	0.7288	0.5052	1.5167
	Ethyl acetate	12.6181	0.9766	13.2268	0.0229	0.0232	0.9399	15.2168	0.0019	0.4241	0.7297	0.7421	2.4437
A-F	n-Hexane	25.9937	0.9837	27.5824	0.0230	0.0373	0.9471	31.7020	0.0009	0.4823	0.7394	1.5477	5.1115
	α-Pinene	41.1105	0.9902	42.3107	0.0260	0.0008	0.9663	47.6405	0.0008	0.2523	0.7322	2.3283	9.2126
	Ethyl acetate	51.2809	0.9960	52.2080	0.0266	0.0032	0.9759	58.8193	0.0006	0.2161	0.7409	2.8817	11.4631
A-B	n-Hexane	14.8124	0.9680	16.2915	0.0218	0.0997	0.9295	18.9275	0.0010	0.7718	0.7339	0.9238	2.7598
	α-Pinene	26.1709	0.9853	27.2163	0.0253	0.0160	0.9575	30.8459	0.0011	0.3191	0.7294	1.5070	5.6948
	Ethyl acetate	36.0263	0.9853	37.0268	0.0252	0.0077	0.9575	41.9659	0.0008	0.2718	0.7293	2.0502	7.7476

* exp: experiment value.
mod: model value.

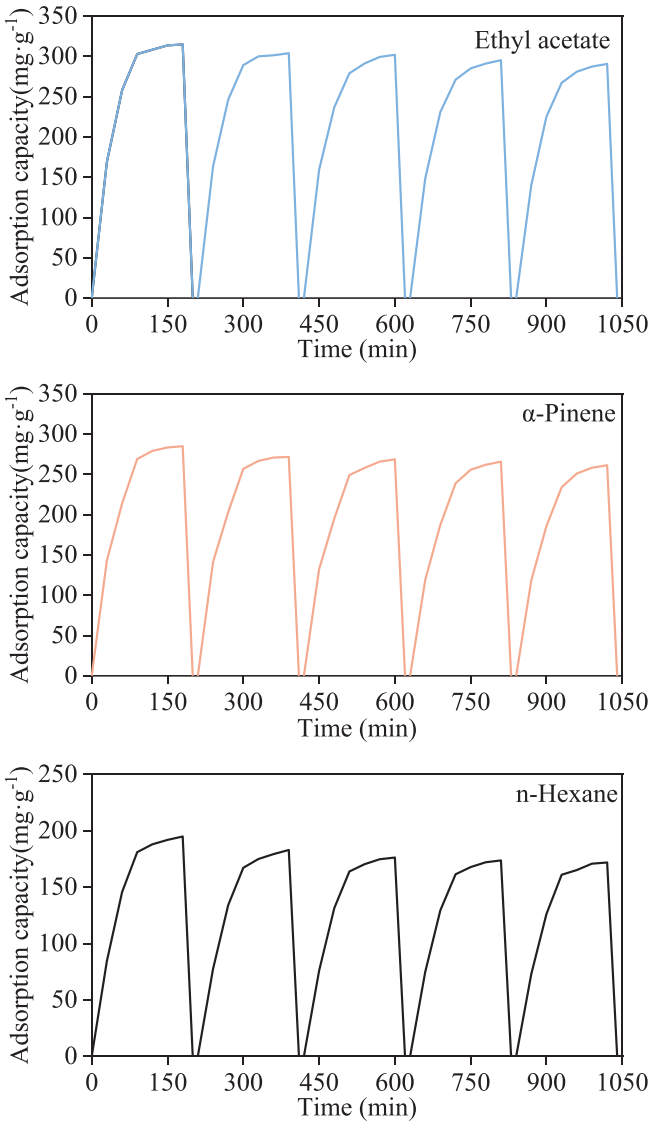

Fig. 5. Five continuous adsorption-desorption of VOCs on the fungal biosorbent A-F.

increasing temperature, but the extent of decrease was less. The reason for the decrease might be a certain chemical adsorption that occurs between the O-F biosorbent and ethyl acetate. In addition, the mass of the these bioadsorbents hardly changed with increasing temperature, because the freeze-drying steps during the preparation of the bioadsorbents could remove most of water from the synthesized biosorbents.

3.5. Reusability

Reusability is an important factor that must be considered when evaluating an adsorbent. Thermal regeneration is a conventional method for the recovery of adsorbate. At high temperature, the adsorbed molecule has enough energy to overcome the van der Waals forces between the adsorbent and adsorbed molecules, making the adsorbed molecule return to the gas phase (Zhou et al., 2012). Several studies showed the desorption temperature was not related to the boiling point of the adsorbed compound (Li et al., 2018), and 373 K was chosen in this study according to technical and economic aspects. To determine the reusability of the synthesized fungal biosorbent A-F, five consecutive VOC sorption-desorption cycles were conducted at 303 and 373 K, respectively, and the results are presented in Fig. 5. After five cycles, the adsorption capacity of fungal biosorbent A-F to ethyl acetate, α-pinene, and n-hexane decreased slightly by 7.64%, 8.01%, and 10.31%, respectively. Interestingly, the largest decline occurred first, whereas slight changes were observed in the next four cycles. There were two reasons for this incomplete desorption, as follows. Formation of permanent bonds and an irreversible transformation of the adsorbed species took place on the adsorbent surface. Some chemically bonded adsorbates that did not desorb blocked the pores and induced the "heel" formation (Auta and Hameed, 2014). The synthetized biosorbent was easily regenerated by heat. Thus, the interaction between the active sites and VOCs on the surface was weak. Such weak bond force suggested that the process was physical adsorption (Balsamo et al., 2013). This result was in agreement with the results obtained from the kinetic study.

Among these synthesized biosorbents, the modified fungal A-F biosorbent demonstrated the best results. The q_{max} value of the A-F biosorbent for VOC adsorption was compared with those of other reported adsorbents. Using ethyl acetate as an example, Xian et al. (2015) used porous material MIL-101 adsorbent, and the q_{max} was 510.16 mg g^{-1}. In the current study, the q_{max} of the A-F biosorbents for ethyl acetate was up to 620.36 mg g^{-1} (Xian et al., 2015). In addition, A-F biosorbents for ethyl acetate exhibited excellent adsorption properties for other hydrophobic VOCs. These values suggested that the synthesized A-F biosorbents have great application potential in VOC adsorption. In addition, the reusability of a biosorbent is also significant in practical applications. Some adsorbents had problems such as incomplete desorption and higher temperatures needed for desorption. For example, after the fifth cycle of palygorskite, the adsorption capacity for 2-heptanone (the desorption temperature is 423 K) decreased by 45.3% (Zhang et al., 2019a). On the basis of better reusability and slight decline of adsorption capacity, the effectiveness of A-F biosorbent as a reusable VOC adsorbent was confirmed. Based on the above discussions, the adsorbent A-F we prepared has good adsorption capacity and high reusability, which means it has great potential in practical applications.

4. Conclusions

The microbial biosorbents for VOC removal were developed in the present study, and most of them exhibited good adsorption properties for VOCs. The aminomethylation-modified fungal (*Ophiostoma* sp. LLC) biosorbent was the best. Surface characteristic analysis and temperature variation on the adsorption capacity showed that the VOC adsorption by these synthesized biosorbents was physical. Such results suggested the potential applicability of this modified fungal biosorbent to VOC purification due to its simple synthesis procedure, high adsorption capacity, and efficient reusability. Meanwhile, this study also provided a novel preparation method for the synthesis of for microbial-based biosorbents.

CRediT authorship contribution statement

Zhuowei Cheng: Conceptualization, Methodology, Investigation, Visualization, Writing - original draft. **Ke Feng:** Validation, Formal analysis, Investigation, Visualization. **Yousheng Su:** Validation, Formal analysis, Visualization. **Jiexu Ye:** Resources, Writing - review & editing. **Dongzhi Chen:** Writing - review & editing, Supervision, Funding acquisition. **Shihan Zhang:** Writing - review & editing. **Xiaomin Zhang:** Investigation. **Dionysios D. Dionysiou:** Writing - review & editing.

Declaration of Competing Interest

The authors declare that they have no known competing financial interests or personal relationships that could have appeared to influence the work reported in this paper.

Acknowledgments

The authors would like to thank the National Key R and D Program of China (grant number 2018YFC0214100), National Natural Science Foundation of China (51678528), the Natural Science Foundation of Zhejiang Province (LY18B060012) and Program for Changjiang Scholars and Innovative Research Team in University (IRT_17R97) provided financial supports to the research. We would like to thank EnPapers (http://www.enpapers.com/enpapers/Index.html) for providing linguistic assistance during the preparation of this manuscript.

Appendix A. Supplementary data

Supplementary data to this article can be found online at https://doi.org/10.1016/j.biortech.2019.122705.

References

Ahmed, I., Jhung, S.H., 2015. Effective adsorptive removal of indole from model fuel using a metal-organic framework functionalized with amino groups. J. Hazard. Mater. 283, 544–550.
Aksu, Z., 2005. Application of biosorption for the removal of organic pollutants: a review. Process Biochem. 40 (3–4), 997–1026.
Aksu, Z., Tezer, S., 2000. Equilibrium and kinetic modelling of biosorption of Remazol Black B by *Rhizopus arrhizus* in a batch system: effect of temperature. Process Biochem. 36 (5), 431–439.
Ammendola, P., Raganati, F., Chirone, R., 2017. CO_2 adsorption on a fine activated carbon in a sound assisted fluidized bed: Thermodynamics and kinetics. Chem. Eng. J. 322, 302–313.
Ashkenazy, R., Gottlieb, L., Yannai, S., 1997. Characterization of acetone-washed yeast biomass functional groups involved in lead biosorption. Biotechnol. Bioeng. 55 (1), 1–10.
Auta, M., Hameed, B.H., 2014. Adsorption of carbon dioxide by diethanolamine activated alumina beads in a fixed bed. Chem. Eng. J. 253, 350–355.
Bai, R.S., Abraham, T.E., 2002. Studies on enhancement of Cr(VI) biosorption by chemically modified biomass of *Rhizopus nigricans*. Water Res. 36 (5), 1224–1236.
Balsamo, M., Budinova, T., Erto, A., Lancia, A., Petrova, B., Petrov, N., Tsyntsarski, B., 2013. CO_2 adsorption onto synthetic activated carbon: Kinetic, thermodynamic and regeneration studies. Sep. Purif. Technol. 116, 214–221.
Bhatnagar, A., Minocha, A.K., Sillanpää, M., 2010. Adsorptive removal of cobalt from aqueous solution by utilizing lemon peel as biosorbent. Biochem. Eng. J. 48 (2), 181–186.
Chen, H., Dai, G., Zhao, J., Zhong, A., Wu, J., Yan, H., 2010. Removal of copper(II) ions by a biosorbent—Cinnamomum camphora leaves powder. J. Hazard. Mater. 177 (1), 228–236.
Chen, H.X., Wang, C.Z., Ye, J.Z., Zhou, H., Tao, R., Li, W.J., 2018. Preparation of starch-hard carbon spherules from ginkgo seeds and their phenol-adsorption characteristics. Molecules 23 (1), 12.
Cheng, Z., Zhang, X., Kennes, C., Chen, J., Chen, D., Ye, J., Zhang, S., Dionysiou, D.D., 2019. Differences of cell surface characteristics between the bacterium *Pseudomonas veronii* and fungus *Ophiostoma stenoceras* and their different adsorption properties to hydrophobic organic compounds. Sci. Total Environ. 650, 2095–2106.
Crini, G., 2006. Non-conventional low-cost adsorbents for dye removal: a review. Bioresour. Technol. 97 (9), 1061–1085.
Dai, H.X., Jing, S.G., Wang, H.L., Ma, Y.G., Li, L., Song, W.M., Kan, H.D., 2017. VOC characteristics and inhalation health risks in newly renovated residences in Shanghai, China. Sci. Total Environ. 577, 73–83.
Daneshvar, E., Vazirzadeh, A., Niazi, A., Sillanpää, M., Bhatnagar, A., 2017. A comparative study of methylene blue biosorption using different modified brown, red and green macroalgae – Effect of pretreatment. Chem. Eng. J. 307, 435–446.
Das, S.K., Ghosh, P., Ghosh, I., Guha, A.K., 2008. Adsorption of rhodamine B on *Rhizopus oryzae*: Role of functional groups and cell wall components. Colloids Surf., B 65 (1), 30–34.
Dhankhar, R., Hooda, A., 2011. Fungal biosorption - an alternative to meet the challenges of heavy metal pollution in aqueous solutions. Environ. Technol. 32 (5), 467–491.
El-Shafey, E.I., Ali, S.N.F., Al-Busafi, S., Al-Lawati, H.A.J., 2016. Preparation and characterization of surface functionalized activated carbons from date palm leaflets and application for methylene blue removal. J. Environ. Chem. Eng. 4 (3), 2713–2724.
Fang, L., Zhou, C., Cai, P., Chen, W., Rong, X., Dai, K., Liang, W., Gu, J.D., Huang, Q., 2011. Binding characteristics of copper and cadmium by cyanobacterium Spirulina platensis. J. Hazard. Mater. 190 (1), 810–815.
Gu, J., Wang, J., Li, Y., Xu, X., Chen, C., Winnubst, L., 2017. Engineering durable hydrophobic surfaces on porous alumina ceramics using in-situ formed inorganic-organic hybrid nanoparticles. J. Eur. Ceram. Soc. 37 (15), 4843–4848.
Huang, J., Liu, D., Lu, J., Wang, H., Wei, X., Liu, J., 2016. Biosorption of reactive black 5 by modified *Aspergillus versicolor* biomass: Kinetics, capacity and mechanism studies. Colloids Surf., A 492, 242–248.
Kim, S.Y., Jin, M.R., Chung, C.H., Yun, Y.S., Jahng, K.Y., Yu, K.Y., 2015. Biosorption of cationic basic dye and cadmium by the novel biosorbent *Bacillus catenulatus* JB-022 strain. J. Biosci. Bioeng. 119 (4), 433–439.
Li, S., Chen, Q., Luo, X., Zhang, W., Zeng, H., 2018. Determination on desorbing temperature of VOCs treated by adsorption method. Focus Air Pollut. Prev. Control 3, 48–50.
Li, Z., Zhu, K., Zhao, Q., Meng, A., 2016. The enhanced SERS effect of Ag/ZnO nanoparticles through surface hydrophobic modification. Appl. Surf. Sci. 377, 23–29.
Liu, H.B., Yang, B., Xue, N.D., 2016. Enhanced adsorption of benzene vapor on granular activated carbon under humid conditions due to shifts in hydrophobicity and total micropore volume. J. Hazard. Mater. 318, 425–432.
Luo, L., Wang, P., Lin, L., Luan, T., Ke, L., Tam, N.F.Y., 2014. Removal and transformation of high molecular weight polycyclic aromatic hydrocarbons in water by live and dead microalgae. Process Biochem. 49 (10), 1723–1732.
Park, D., Yun, Y.S., Park, J.M., 2010. The past, present, and future trends of biosorption. Biotechnol. Bioprocess Eng. 15 (1), 86–102.
Park, D., Yun, Y.S., Park, J.M., 2005. Studies on hexavalent chromium biosorption by chemically-treated biomass of *Ecklonia sp*. Chemosphere 60 (10), 1356–1364.
Qiu, W., Dou, K., Zhou, Y., Huang, H., Chen, Y., Lu, H., 2018. Hierarchical pore structure of activated carbon fabricated by CO_2/microwave for volatile organic compounds adsorption. Chin. J. Chem. Eng. 26 (1), 81–88.
Ramrakhiani, L., Majumder, R., Khowala, S., 2011. Removal of hexavalent chromium by heat inactivated fungal biomass of *Termitomyces clypeatus*: Surface characterization and mechanism of biosorption. Chem. Eng. J. 171 (3), 1060–1068.
Shafiei, M., Alivand, M.S., Rashidi, A., Samimi, A., Mohebbi-Kalhori, D., 2018. Synthesis and adsorption performance of a modified micro-mesoporous MIL-101(Cr) for VOCs removal at ambient conditions. Chem. Eng. J. 341, 164–174.
Shen, Y., Zhang, N., 2019. Facile synthesis of porous carbons from silica-rich rice husk char for volatile organic compounds (VOCs) sorption. Bioresour. Technol. 282, 294–300.
Sheng, G.-P., Yu, H.Q., Li, X.Y., 2010. Extracellular polymeric substances (EPS) of microbial aggregates in biological wastewater treatment systems: a review. Biotechnol. Adv. 28 (6), 882–894.
Song, G., Zhu, X., Chen, R., Liao, Q., Ding, Y.-D., Chen, L., 2016. An investigation of CO_2 adsorption kinetics on porous magnesium oxide. Chem. Eng. J. 283, 175–183.
Sugimoto, I., Nagaoka, T., Seyama, M., Nakamura, M., Takahashi, K., 2007. Classification and characterization of atmospheric VOCs based on sorption/desorption behaviors of plasma polymer films. Sens. Actuators B 124 (1), 53–61.
Vijayaraghavan, K., Yun, Y.S., 2008. Bacterial biosorbents and biosorption. Biotechnol. Adv. 26 (3), 266–291.
Wang, N., Qiu, Y., Xiao, T., Wang, J., Chen, Y., Xu, X., Kang, Z., Fan, L., Yu, H., 2019. Comparative studies on Pb(II) biosorption with three spongy microbe-based biosorbents: High performance, selectivity and application. J. Hazard. Mater. 373, 39–49.
Wang, S., Liu, C., Liu, G., Zhang, M., Li, J., Wang, C., 2011. Fabrication of super-hydrophobic wood surface by a sol–gel process. Appl. Surf. Sci. 258 (2), 806–810.
Wang, X., Zheng, X., Shen, Y., Wang, T., 2017. Biosorption kinetics and mechanisms of low concentration uranium by live and heat-killed Saccharomyces cerevisiae. Acta Scientiae Circumstantiae 37 (1), 169–177.
Xian, S.K., Yu, Y., Xiao, J., Zhang, Z.J., Xia, Q.B., Wang, H.H., Li, Z., 2015. Competitive adsorption of water vapor with VOCs dichloroethane, ethyl acetate and benzene on MIL-101(Cr) in humid atmosphere. RSC Adv. 5 (3), 1827–1834.
Yee, N., Benning, L.G., Phoenix, V.R., Ferris, F.G., 2004. Characterization of metal-cyanobacteria sorption reactions: A combined macroscopic and infrared spectroscopic investigation. Environ. Sci. Technol. 38 (3), 775–782.
Yu, Y., Qiao, N., Wang, D., Zhu, Q., Fu, F., Cao, R., Wang, R., Liu, W., Xu, B., 2019. Fluffy honeycomb-like activated carbon from popcorn with high surface area and well-developed porosity for ultra-high efficiency adsorption of organic dyes. Bioresour. Technol. 285, 121340.
Yun, Y.S., Park, D., Park, J.M., Volesky, B., 2001. Biosorption of trivalent chromium on the brown seaweed biomass. Environ. Sci. Technol. 35 (21), 4353–4358.
Zhang, G., Feizbakhshan, M., Zheng, S., Hashisho, Z., Sun, Z., Liu, Y., 2019a. Effects of properties of minerals adsorbents for the adsorption and desorption of volatile organic compounds (VOC). Appl. Clay Sci. 173, 88–96.
Zhang, L., Wu, Y., Zhang, L., Wang, Y., Li, M., 2016a. Synthesis and characterization of mesoporous alumina with high specific area via coprecipitation method. Vacuum 133, 1–6.
Zhang, P., Li, Y., Cao, Y., Han, L., 2019b. Characteristics of tetracycline adsorption by cow manure biochar prepared at different pyrolysis temperatures. Bioresour. Technol. 285, 121348.
Zhang, X., Gao, B., Zheng, Y., Hu, X., Creamer, A.E., Annable, M.D., Li, Y., 2017. Biochar for volatile organic compound (VOC) removal: Sorption performance and governing mechanisms. Bioresour. Technol. 245, 606–614.
Zhang, X., Yang, C.W., Yu, H.Q., Sheng, G.P., 2016b. Light-induced reduction of silver ions to silver nanoparticles in aquatic environments by microbial extracellular polymeric substances (EPS). Water Res. 106, 242–248.
Zhou, X., Yi, H., Tang, X., Deng, H., Liu, H., 2012. Thermodynamics for the adsorption of SO_2, NO and CO_2 from flue gas on activated carbon fiber. Chem. Eng. J. 200–202, 399–404.
Zou, W., Gao, B., Ok, Y.S., Dong, L., 2019. Integrated adsorption and photocatalytic degradation of volatile organic compounds (VOCs) using carbon-based nanocomposites: A critical review. Chemosphere 218, 845–859.